The DØ upgrade

Mitchell R. Wayne*

Department of Physics, University of Notre Dame, Notre Dame, IN 46556, USA

For the DØ Collaboration

Abstract

The DØ detector is undergoing a major upgrade to prepare for Run II with the Main Injector at the Fermilab collider. Key elements of the upgrade include a new, magnetic tracking system containing a silicon vertex detector and scintillating fiber outer tracker inside a 2 T field. The upgrades will increase the physics reach of the DØ experiment in several areas, including the study of the physics of the b-quark. In particular, simulation studies show that a measurement of $\sin 2\beta$ can be made with an uncertainty of order 0.15, and that by fully reconstructing decays of the B_s, values of $x_s \leq 20$ can be resolved. © 1998 Elsevier Science B.V. All rights reserved.

1. Introduction

A new collider run at the Fermilab Tevatron, known as Run II, will begin early in the year 2000. The addition of the Main Injector will enable the accelerator to significantly increase the integrated luminosity delivered to the experiments. It is expected that both DØ and CDF will accumulate on the order of 1 fb^{-1} of data per year, to be compared to the total of approximately 120 pb^{-1} collected during all of Run I. To achieve this, the instantaneous luminosity at the Tevatron will reach 2×10^{32}/cm^2/s, and the time between bunch crossings will decrease to 396 ns, and eventually to 132 ns.

The improvement of the accelerator provides two strong motivating factors for upgrading the existing DØ detector. First, the detector must be improved to take full advantage of the physics opportunities afforded by the large increase in integrated luminosity. Second, the upgraded DØ detector must be able to function well in the more difficult operating conditions brought about by the increased instantaneous luminosity and the decreased bunch crossing times of Run II.

The DØ detector upgrades underway should satisfy both of these goals. The upgrade preserves the strengths of the current detector, in particular the excellent calorimeter coverage, while at the same time strongly enhances the tracking and triggering capabilities. The Run I DØ tracking system inside the calorimeter is being entirely replaced by a new tracker situated within a 2.0 T solenoidal field. While the central and end-cap calorimeters remain unchanged, their readout electronics will be improved for the shorter bunch crossing times. In the muon system, a combination of new tracking detectors, trigger counters and improved electronics will strengthen the region $|\eta| \leq 2$. Finally, a new

* E-mail: wayne@undhep.hep.nd.edu.

3-level, buffered trigger system incorporating many of the new detector systems will handle the higher rates of Run II.

2. Overview of upgrade tracking

A very significant part of the DØ upgrade is a new, magnetic tracking system which will completely replace the existing tracker. A schematic view of the upgrade tracker is shown in Fig. 1.

2.1. Silicon vertex detector

In the region just outside the beam pipe, a silicon vertex detector will provide precision tracking of charged particles and measurements of both primary and secondary vertices. The silicon detector is an integrated system of barrels and disks designed to provide tracking over a large range of pseudorapidity [1]. The barrels are segmented into six sections along the beam direction, with four radial layers in each segment. The innermost and third barrel have double-sided detectors with axial and 90° stereo strips in the four central segments. The outer two segments are single-sided detectors with axial strips only. The second and fourth barrels contain double-sided detectors with axial and 2° stereo strips throughout. Including both barrels and disks, the silicon tracker contains more than 800 000 channels.

A beam test of a number of both single-sided and double-sided silicon detectors was carried out in summer 1997 at Fermilab. The detectors were read out with the SVXIIe chip and the system was run at the nominal operating rate of 53 MHz. The test apparatus included a small 2 T magnet so that the performance of the detectors could be studied in a variety of orientations with respect to the magnetic field. Fig. 2 shows a plot of residuals for a typical detector. After corrections for multiple scattering and alignment errors, the measured sigma of
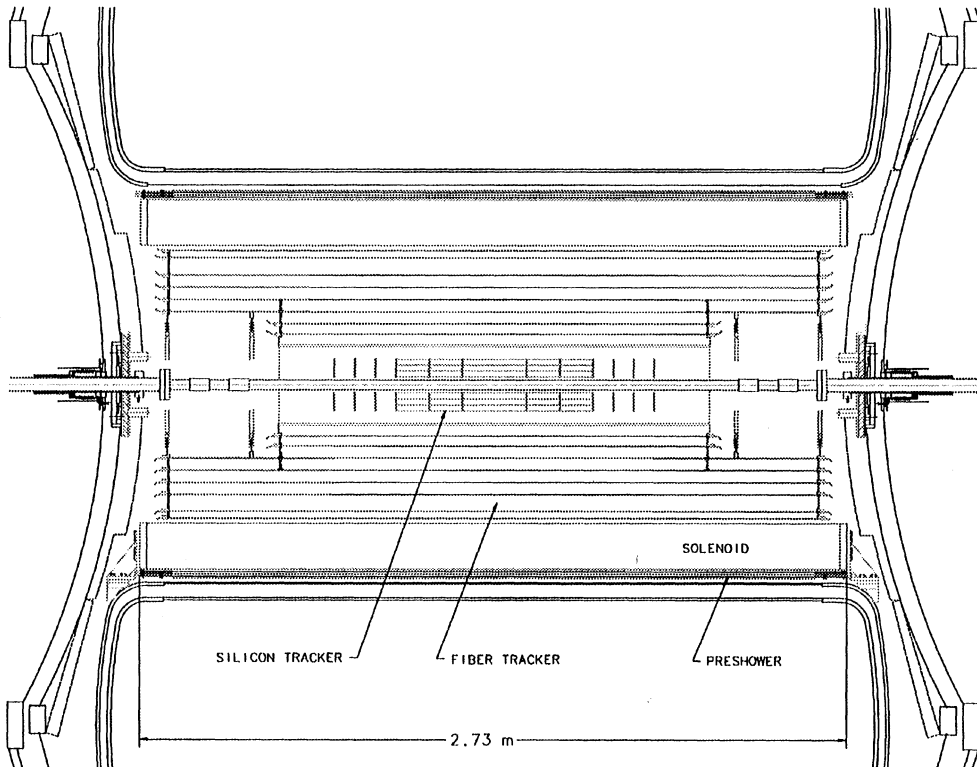

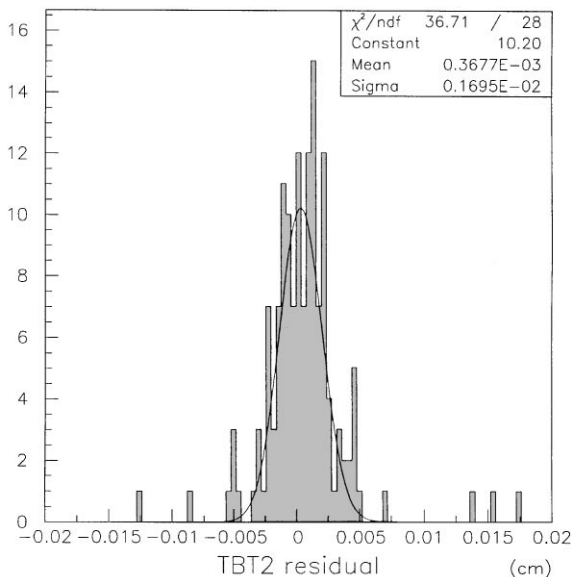Fig. 1. Schematic view of the DØ upgrade tracking system.

Fig. 2. Residual plot for a silicon detector in the test beam.

Fig. 3. Charge cluster plots for a silicon detector irradiated to 1 MRad (above) and for a non-irradiated detector (below).

17 μm is reduced to less than 10 μm, close to the expected resolution. In Fig. 3, the response of a silicon detector irradiated to 1 Mrad is compared to a non-irradiated detector. The irradiated detector clearly is still a useable device, although it requires a higher operating bias and has a mean cluster charge reduced by about 30%. This result indicates that even the innermost layer of the silicon detector should survive the total expected radiation damage at Run II.

2.2. Central fiber tracker

Surrounding the silicon vertex detector is the central fiber tracker [2]. This detector is made up of eight concentric cylinders of scintillating fibers, ranging in radius from 20 to 50 cm. The cylinders are about 2.5 m in length except for the inner two, which are about 1.7 m long. Each cylinder contains a doublet layer of axial fibers along with a second doublet layer of either u or v 2° stereo fibers on successive cylinders. Each scintillating fiber is mated to a long, clear optical fiber which transports the scintillation light to a Visible Light Photon Counter (VLPC), a new solid-state photodetector developed for this detector [3]. The VLPC provides the fiber tracker with a photodetector having
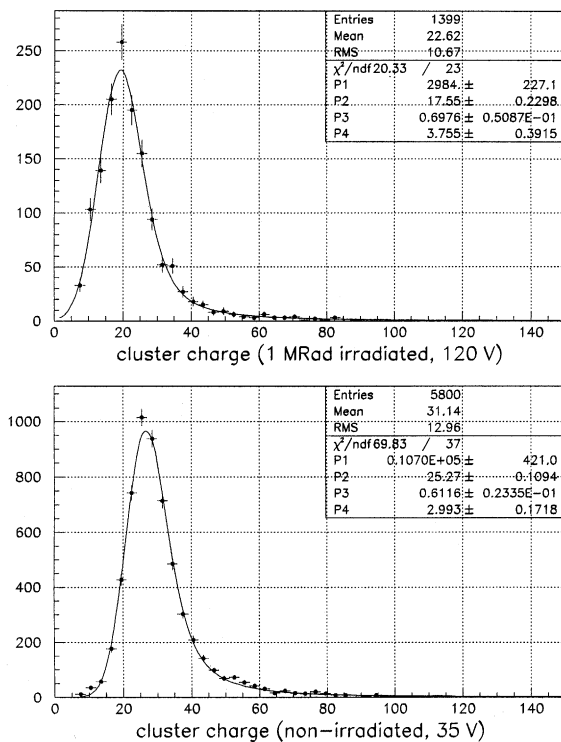
excellent quantum efficiency and gain (on the order of 80% and 50 000 respectively). The tracker contains approximately 78 000 channels in total.

Fig. 4 shows the elements making up a single channel of the central fiber tracker. Both the scintillating and clear waveguide fibers are 830 μm in diameter. They are multiclad fibers with a polystyrene core. The active fibers are mirrored at the non-readout end, and mated to the clear fiber through connectors at the readout end of the support cylinder. The scintillation light is brought to cryogenic "cassettes", each of which contain a total of 1024 VLPC pixels in 128, eight-pixel arrays. The cryogenic system is required to maintain the VLPCs at an operating temperature of about 9 K. The VLPC output is sent via a kapton flex circuit to a front-end amplifier and then on to the same SVXIIe chip used to read out the silicon vertex detector.

A 3024 channel prototype of the fiber tracker took data in a cosmic ray test for nearly a year of
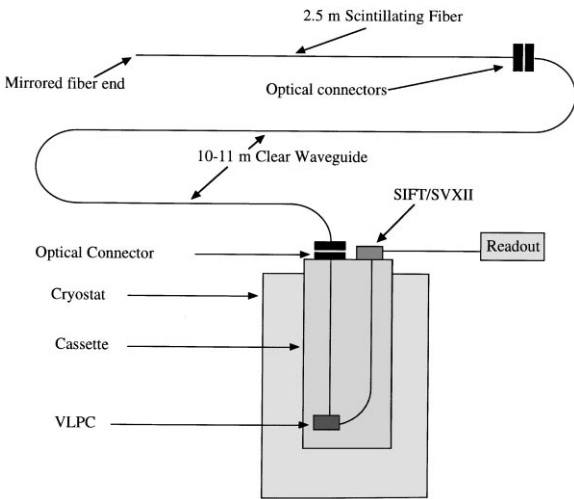
Fig. 4. The elements of a single channel of the Central Fiber Tracker.

running in 1994–1995. The position resolution measured for the doublet layers was of order 100 μm, in line with expectations. With a configuration of fiber lengths comparable to that of the final detector, a mean of about nine photoelectrons per fiber was detected for minimum ionizing cosmic rays. A typical threshold was just under 1.0 photoelectron, leading to a doublet layer efficiency of ≥ 99.5%. Accounting for improvements in the fiber quality, connectors and VLPC quantum efficiency since the cosmic ray test, it is expected that for the final detector a mean of 12 photoelectrons per fiber will be detected in the "worst case", namely for a track crossing at normal incidence in the middle of a scintillating fiber. This high photo-yield should give a doublet layer efficiency of nearly unity, making the fiber tracker very efficient for both tracking and triggering.

2.3. Solenoid

Both the silicon vertex detector and the scintillating fiber tracker are situated within a 2.0 T superconducting solenoid. The solenoid has an inner radius of 53 cm, an outer radius of 72 cm and is 2.8 m long. The magnet has been tested at full field and it is presently at DØ awaiting installation in the detector.

2.4. Central and forward preshower

The central preshower detector sits in the small radial gap between the outside wall of the solenoid and the inside of the central calorimeter. This detector will help regain any loss in calorimeter energy resolution that the addition of the solenoid might produce, and will also aid in triggering on electrons. The central preshower is made up of layers of triangular-shaped extruded strips of scintillator, with a wavelength-shifting fiber running down the center of each strip. These fibers are mated to clear fibers which also transport the light to Visible Light Photon Counters. A small prototype of the central preshower was tested in the same cosmic ray test stand used for the fiber tracker. The measured light output and position resolution for MIPs was as expected [4]. Forward preshower detectors based on the same technology will also be mounted on the front face of each of the endcap calorimeters.

2.5. Upgrade tracker performance

The expected performance of the DØ upgrade tracking system is illustrated in Figs. 5 and 6. In Fig. 5, the transverse momentum resolution is shown as a function of η for four different values of P_T. Fig. 6 shows the two-dimensional impact parameter resolution for tracks at $\eta = 0$ as a function of transverse momentum. The two curves show the resolution for the silicon detector alone and for the silicon and fiber trackers combined.

3. Physics potential of the DØ upgrade

The upgrades described above will make the DØ detector a powerful instrument for doing the physics of Run II [5]. Some of the features that the upgrade will provide are the ability to tag b-quark decays via displaced vertices, enhanced ability to identify and trigger on both electrons and muons, and the ability to determine the sign of charged particles. These features will allow DØ to study a wide range of physics, including: the study of large samples of top quarks, W and Z bosons, which will provide precision tests of the Standard Model and further constraints on the mass of a Higgs boson;
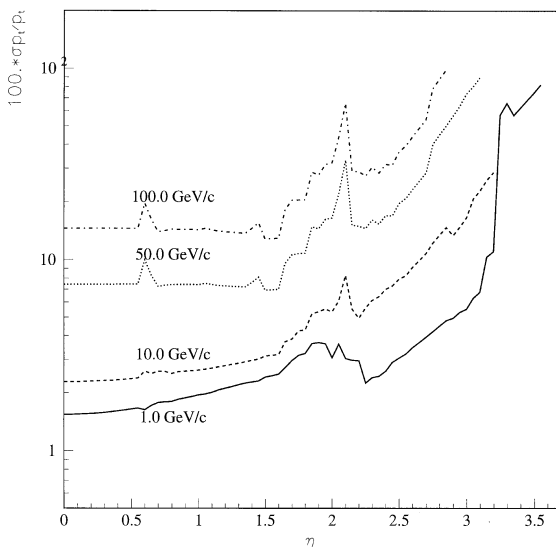
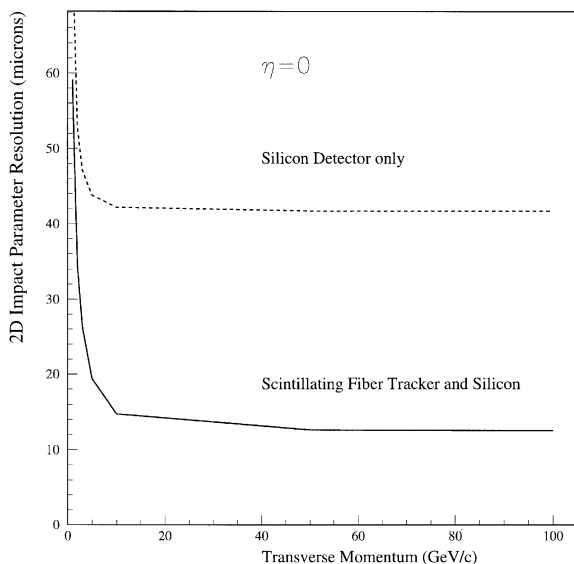Fig. 5. Transverse momentum resolution of the tracker as a function of pseudorapidity for several momenta.

Fig. 6. Two-dimensional impact parameter resolution for tracks at $\eta = 0$ as a function of transverse momentum. The two curves show the result for the silicon detector alone (dashed line) and for the silicon and fiber trackers together (solid line).

accurate measurements of many aspects of QCD, improving the already significant DØ program in this area; the study of the production and decay of b-quark hadrons; and of course the search for physics beyond the Standard Model.

Several features of the upgrade will improve DØ's ability to study the top quark in Run II, the most significant of which comes from the tagging of secondary vertices from b-quark decays. Fig. 7 shows a Monte Carlo simulation of the signed impact parameter measured for b-quark jets, compared with a background of W + 4 jet events. It is estimated that the probability to tag at least one b-quark jet from a $t\bar{t}$ event will be greater than 80%, and both jets can be tagged with about 50% efficiency. Along with the improvements in lepton identification and momentum resolution, it is expected that DØ will measure the top quark mass to a precision of 4 GeV in Run II.

In the area of electroweak physics, a key measurement will be an accurate determination of the W boson mass. Along with improved statistics, the upgraded detector will be able to reduce many of the systematic errors in the current measurement. It is anticipated that, with an integrated luminosity of 1 fb^{-1}, DØ will measure the mass of the W to within 50 MeV.

4. B physics at Run II

The detector upgrades will greatly improve the DØ ability to study the physics of the b-quark. The very large $b\bar{b}$ production cross section will enable the search for rare decays of b hadrons. The ability to tag b-quarks and measure their decay vertices will allow DØ to make two important measurements in Run II.

4.1. CP violation

First, it is predicted that CP violation will be observed in the beauty system in the form of an asymmetry $A_{CP} = (N - \bar{N})/(N + \bar{N})$ where $N(\bar{N})$ is the number of $B^0(\bar{B}^0)$ decaying to the final state ψK_s. This asymmetry is used to measure $\sin 2\beta$, where β is one of the angles in the CKM unitarity triangle. To measure the asymmetry requires reconstructing the ψK_s final state from one B hadron and flavor tagging the other, generally by measuring the sign of a decay muon or electron. The experimentally observed asymmetry is diluted and is given by $A_{obs} = D A_{CP}$, with $D = d_1 d_2 d_3$. The three dilution factors come from the following sources:
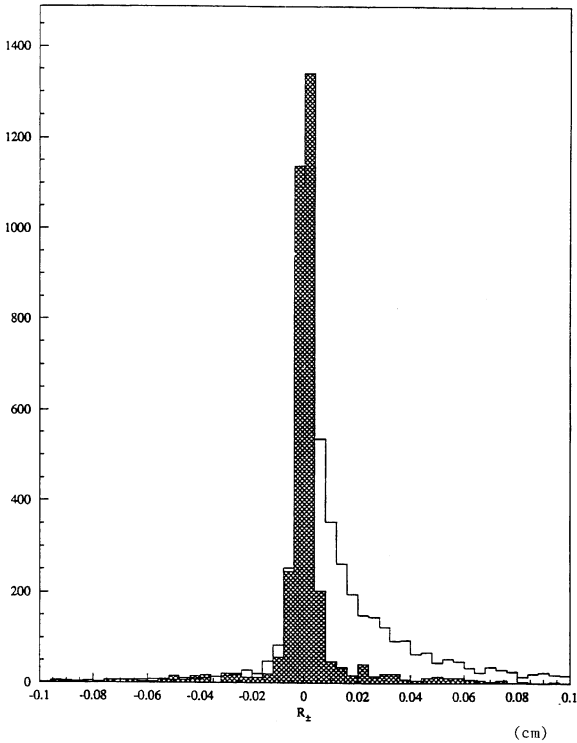
Fig. 7. Signed impact parameter for b-quark decays from t$\bar{\text{t}}$ events (open histogram) and for a background of W + 4 jet events (shaded histogram).

Fig. 8. Reconstructed invariant mass plots for $\psi \to \mu\mu$ and for $B^0 \to \psi K_s$.

d_1 from mixing in the "signal" side before the B hadron decays to ψK_s; d_2 accounts for flavor mistagging of the other B hadron; and d_3 is from backgrounds in the signal sample.

To determine the DØ detector's sensitivity to this asymmetry a simulation was carried out in which the flavor tagging was limited to muons and the decay of the ψ was restricted to di-muons [6]. Fig. 8 shows the reconstructed mass plots for the ψ and subsequent B^0, with resolutions of 30 and 40 MeV, respectively. After all the trigger and reconstruction cuts, it is estimated that for an integrated luminosity of $2\,\text{fb}^{-1}$ DØ will see a total signal $N_{\text{obs}} = 1340\varepsilon$ reconstructed and tagged events, where ε includes any extra trigger or reconstruction inefficiencies not in the current simulations.

We estimate the total dilution factor in the following way [6]. The effect of mixing on the signal side, d_1 comes from the time integrated nature of the measurement where decays are counted irre-
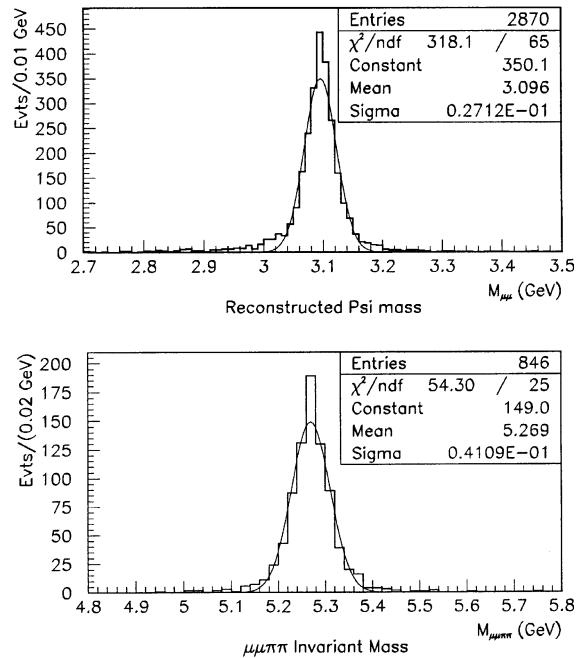
spective of decay length. It is calculated to have a value of 0.46 using the value $x_d = 0.66$ as input. A decay length cut is expected to have very little impact on this value. The flavor mistagging can come from several sources which combine to give an estimated value of $d_2 = 0.5$. Finally, assuming a signal to background ratio of 2/1, d_3 is estimated to be 0.8. These three factors combine to give a total dilution factor of $D \simeq 0.2$.

The sensitivity to CP violation is then given by $\delta(\sin 2\beta) = 1/D\sqrt{N_{\text{obs}}}$. Given the values above for the expected signal and dilution factors, the error on $\sin 2\beta$ becomes $\delta(\sin 2\beta) \simeq 0.15/\sqrt{\varepsilon}$. It is reasonable to expect $90\% \geq \varepsilon \geq 60\%$, which would correspond to $0.15 \leq \delta(\sin 2\beta) \leq 0.19$. It should be noted that this error can be improved by adding in the di-electron decays of the ψ and by including electron flavor tags of the other B hadron, but these simulation studies have not yet been carried out.

4.2. B_s mixing

The DØ experiment will also be able to either observe or set a limit on the mixing of the neutral
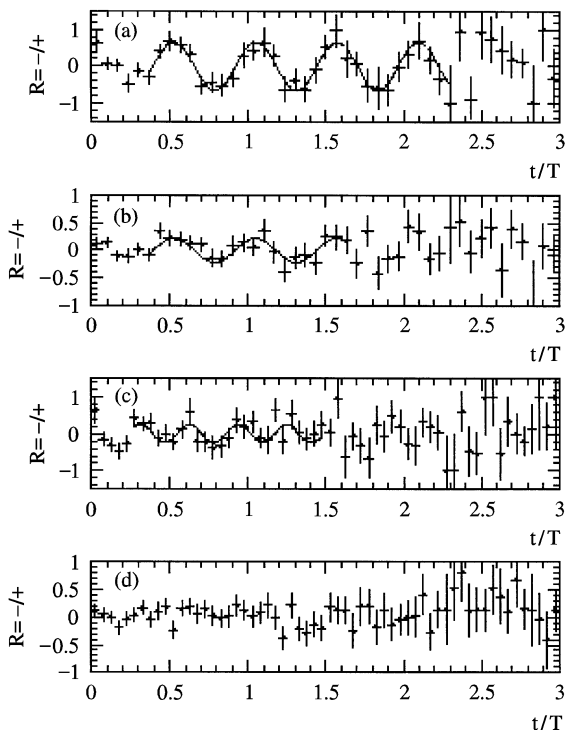
Fig. 9. Ratio of mixed to non-mixed events for $B_s \rightarrow D_s\pi, D_s3\pi$. Figures (a) and (c) are for input values of $x_s = 12$ and 20 with perfect tagging and no background. Figures (b) and (d) are for the same two values of x_s but with a 25% mistagging probability and $S/B = 1/1$.

B_s hadron [7]. The mixing parameter x_s can be determined by measuring the difference of mixed and non-mixed events as a function of proper time. The measurement requires good secondary vertex resolution, and hence good resolution on the B_s lifetime. This can be achieved at DØ by fully reconstructing $B_s \rightarrow D_s\pi, D_s3\pi$, with $D_s \rightarrow \phi\pi$. A decay muon from the other B hadron provides a flavor tag for the event.

A Monte Carlo simulation of this strategy has been carried out at DØ. The study predicts on the order of 2000 fully reconstructible B_s decays with an oppposite side muon flavor tag in $2\,\text{fb}^{-1}$. This sample will be reduced somewhat due to offline reconstruction losses. The sensity to x_s for a sample of 1000 events is shown in Fig. 9, which plots the

ratio of mixed to unmixed events as a function of proper time. Fig. 9a and Fig. 9c correspond to input values for x_s of 12 and 20, respectively, and are for ideal tagging and no backgrounds. Fig. 9b and Fig. 9d are for the same two values of x_s, but with the introduction of a 25% mistagging rate and a signal to background ratio of 1/1. The results of these studies indicate that DØ should be sensitive to x_s values up to about 20, and perhaps as high as 25.

5. Summary

An extensive upgrade of the DØ detector is well underway in preparation for Run II at the Fermilab Tevatron. The upgrade features a completely new magnetic tracking system which will provide precision tracking, momentum measurement and sign determination for charged particles, and track triggering. The improved detector, along with the upgraded accelerator, will enable DØ to study a broad range of physics topics. In the area of b-quark physics, DØ will be able to determine $\sin 2\beta$ to within an error of about 0.15, and will be sensitive to x_s values up to the range of 20–25.

References

[1] R. Lipton, Nucl. Instr. and Meth. A 386 (1997) 96; DØ Note 2542 (1995).
[2] DØ Note 2542 (1995); G. Guttierez, Proc. SciFi97: Conf. on Scintillating and Fiber Detectors, A.D. Bross, R.C. Ruchti, M.R. Wayne (Eds.), AIP Conf. Proc., to be published.
[3] M.D. Petroff, M.G. Stapelbroek, IEEE Trans. Nucl. Sci. NS-36 (1989) 158; M.D. Petroff, M. Atac, IEEE Trans. Nucl. Sci. NS-36 (1989) 163; M.R. Wayne, Nucl. Instr. and Meth. A 387 (1997) 278.
[4] M. Adams et al., Nucl. Instr. and Meth. A 366 (1995) 263; M. Adams et al., Nucl. Instr. and Meth. A 378 (1996) 131.
[5] R.C. Ruchti, Proc. 10th Topical Workshop on Proton–Antiproton Collider Physics, AIP Conf. Proc. 357 (1996) 421; The DØ Collaboration, Proc. Int. Europhysics Conf. on High Energy Physics, 1997, to be published.
[6] G. Lima, A. Maciel, DØ Note 3228.
[7] A. Maciel, Proc. 2nd Int. Conf. on B Physics and CP Violation, 1997, to be published.